

# TRIGGERED STAR FORMATION ON THE BORDER OF THE ORION-ERIDANUS SUPERBUBBLE

Hsu-Tai Lee<sup>1,2</sup>

htlee@asiaa.sinica.edu.tw

W. P. Chen<sup>1,3</sup>

wchen@astro.ncu.edu.tw

## ABSTRACT

A census of classical T Tauri stars and Herbig Ae/Be stars has been performed around the Orion-Eridanus Superbubble which is ionized and created by the Ori OB1 association. This sample is used to study the spatial distribution of newborn stars, hence the recent star formation sequence, in the region that includes two giant molecular clouds (Orion A and B) and additional smaller clouds (NGC 2149, GN 05.51.4, VdB 64, the Crossbones, the Northern Filament, LDN 1551, LDN 1558, and LDN 1563). Most of the molecular clouds are located on the border of the Superbubble, and associated with  $H\alpha$  filaments and star formation activity, except the Northern Filament which is probably located outside the Superbubble. This suggests that while star formation progresses from the oldest Ori OB1a subgroup to 1b, 1c and 1d, the Superbubble compresses and initiates starbirth in clouds such as NGC 2149, GN 05.51.4, VdB 64, and the Crossbones, which are located more than one hundred pc away from the center of the Superbubble, and even in clouds some two hundred pc away, i.e., in LDN 1551, LDN 1558, and LDN 1563. A superbubble appears to have potentially a long-range influence in triggering next-generation star formation in an OB association.

*Subject headings:* stars: formation — stars: pre-main-sequence — ISM: clouds — ISM: molecules

---

<sup>1</sup>Institute of Astronomy, National Central University, Taiwan 320, R.O.C.

<sup>2</sup>Institute of Astronomy and Astrophysics, Academia Sinica, P.O. Box 23–141, Taipei 10617, Taiwan, R.O.C.

<sup>3</sup>Department of Physics, National Central University, Taiwan, 320, R.O.C.

## 1. INTRODUCTION

Ori OB1 is one of the nearest OB associations (de Zeeuw et al. 1999), harboring some 10 O-type stars (Humphreys 1978). Blaauw (1964) divides the Ori OB1 association into four subgroups, Ori OB1a, 1b, 1c, and 1d, with 1a being the oldest and 1d (the Orion Nebula) being the youngest (Brown et al. 1994; Warren & Hesser 1978; Blaauw 1991). From the *Hipparcos* catalogue, de Zeeuw et al. (1999) determine distances of  $336\pm 16$ ,  $473\pm 33$ , and  $506\pm 37$  pc to Ori OB1a, 1b, and 1c, respectively.

In Ori OB1, most of the current star formation activity is located in, or close to, the two giant molecular clouds (Walter et al. 2000; Megeath et al. 2005; Hernández et al. 2007a; Briceño et al. 2007a), Orion A and B, which have been surveyed in  $^{12}\text{CO}$  by Maddalena et al. (1986) and Wilson et al. (2005). Together with many smaller molecular clouds, the entire region is called the Orion-Monoceros complex (Maddalena et al. 1986; Wilson et al. 2005).

As the Ori OB1 association evolved, the ionization photons and stellar winds from massive stars and supernova ejectra produced the Orion-Eridanus Superbubble (Brown et al. 1995). The Orion-Eridanus Superbubble has been studied in many wavelengths (reviews by Heiles et al. 1999), e.g., in H I (Heiles 1976; Brown et al. 1995), *IRAS*  $100\ \mu\text{m}$  (Burrows et al. 1993),  $\text{H}\alpha$  (Sivan 1974; Reynolds & Ogden 1979), X rays (Burrows et al. 1993; Snowden et al. 1995; Guo et al. 1995), and  $\gamma$  rays (Parizot 1998).

Even though the Orion-Eridanus Superbubble is one of the most explored superbubbles, the overall star formation related to the Superbubble is not well investigated, simply because of its large sky coverage. It is indeed a great challenge to identify low-mass pre-main-sequence (PMS) stars in such a large region, so a wide-field survey is needed. Walter et al. (2000) and Briceño et al. (2007a) summarize different methods to search for low-mass ( $0.1\text{--}1\ M_{\odot}$ ) PMS stars in OB associations, e.g., by objective-prisms, X rays, proper motions, and variability surveys. Each method has its own advantage and drawback and here we summarize briefly each of the methods that have been applied to the Orion region.

An objective-prism imaging finds emission-line stars as young star candidates. A large number of candidate PMS stars have been recognized by this method, e.g., in Orion (Wiramihardja et al. 1989, 1991, 1993; Kogure et al. 1989) by the Kiso  $\text{H}\alpha$  survey. The total number of  $\text{H}\alpha$  emission stars is 1157 over an area of 150 square degrees (Wiramihardja et al. 1993) to a limiting magnitude of  $V=15$ . However, an  $\text{H}\alpha$  survey detects PMS stars only with strong  $\text{H}\alpha$  emission, i.e., classical T Tauri stars (CTTSs) and Herbig Ae/Be (HAeBe) stars, but is not sensitive to weak-line T Tauri stars (WTTSs). An object-prism sample may also be contaminated considerably by late-type dwarfs that also show  $\text{H}\alpha$  in emission, namely the dMe stars. Indeed, Briceño et al. (2001) conclude that only about 40% of the  $\text{H}\alpha$  emission stars

in Orion OB1a found in the Kiso H $\alpha$  survey are really PMS stars.

Because low-mass PMS stars (CTTSs and WTTSs) are X-ray sources (Feigelson & Montmerle 1999), the *ROSAT* All Sky Survey (RASS), for example, has been used for large-scale searches for low-mass PMS stars. *ROSAT* is sensitive to soft X rays, so would find preferentially WTTSs. The main contaminations in an RASS sample would be chromospherically active K and M dwarfs. Sterzik et al. (1995) study the density distribution of X-ray-selected PMS candidate stars in Ori OB1 (700 square degrees) and find significant surface density enhancements around Ori OB1a, OB1b, OB1c, and  $\lambda$  Ori. Alcalá et al. (1996) accomplish spectroscopic and photometric observations of the RASS X-ray sources in the Orion cloud complex and find 112 new WTTSs in about 450 square degrees, and follow up by broad- and narrow-band photometric and high-resolution spectroscopic observations (Alcalá et al. 1998, 2000). Walter et al. (2000) compare the spatial distributions of the H $\alpha$  emission stars in the Kiso H $\alpha$  survey and RASS X-ray sources in Ori OB1. The H $\alpha$  emission line sources (CTTSs) are spatially closer to the Orion molecular clouds than the X-ray sources (WTTSs), a consequence of CTTSs being less evolved than WTTSs so are still in the proximity of their birthplace.

Stars in an OB association share common space motions, so proper-motion measurements can be used to identify probable members in an OB association with no limitation on stellar masses. Because it is difficult to measure accurately proper motions of faint stars, this method is restricted to nearby OB associations and bright (massive and intermediate-mass) stars (de Zeeuw et al. 1999). One vulnerability of this technique is that the proper motions near the solar apex or antapex are small, so it is unsuitable to study regions near these two directions, as is the case for Ori OB1 which is close to the solar antapex.

PMS stars are variable (Herbst et al. 1994), so a multi-epoch photometric monitoring can be used to identify possible PMS stars in an OB association. This method ensures that most PMS stars be found, but may also pick up other kinds of variables which are difficult to weed out on the basis of variability alone. However, to conduct a multi-epoch survey of a large region is time-consuming. Using this method, Briceño et al. (2005) have identified 56 low-mass young stars in the Ori OB1a subgroup, and 141 in Ori OB1b. Recently, Briceño et al. (2007b) apply a similar method and find nearly 200 low-mass PMS stars in the 25 Ori group. Carpenter et al. (2001) use the southern 2MASS telescope and perform a  $0.84 \times 6$  square degrees multi-epoch photometric observations near Trapezium. They find 1235 near-infrared variable stars, most of which ( $\sim 93\%$ ) are probably associated with the Orion A molecular cloud. They also show that the spatial distribution of stars with near-infrared excess traces the  $^{13}\text{CO}$  emission well.

None of the methods mentioned above are sensitive to those young stars embedded in

clouds because of excessive extinction. Recently, *Spitzer Space Telescope* is used to investigate disk evolution in the  $\sigma$  Orionis cluster, 25 Orionis aggregate in Ori OB1a, and Ori OB1b (Hernández et al. 2007a,b). Megeath et al. (2005) conduct a survey in the Orion region with *Spitzer* to study star formation associated with the A and B molecular clouds.

In this work, we use 2MASS near-infrared data (Cutri et al. 2003) to select CTTSs and HAeBe stars, so as to diagnose recent star formation related to the Superbubble. Although near-infrared data miss sources deeply inside a cloud, most CTTSs and HAeBe stars can still be detected in the region we have investigated. We describe in §2 selection criteria of the young star sample, and follow-up spectroscopic observations. In §3, we outline the properties of some specific star-forming regions. We discuss in §4 the structure of the Superbubble, and how it influences the star formation history out to a distance of some 200 pc. The conclusions are summarized in §5.

## 2. OBSERVATIONS AND RESULTS

### 2.1. Selection of PMS Candidate Stars

Existence of young stellar objects indicates star formation activity in a molecular cloud. The time scales (or ages) of protostars are short ( $\sim 10^5$  yr), so the chances of finding protostars in a cloud are low even if the cloud has ongoing star formation. On the other hand, the number of PMS stars, with an order of longer evolutionary time scales, should be much higher. CTTSs in general are in an earlier evolutionary stage — hence in closer spatial association with molecular clouds — than the WTTS population, which usually has an extended spatial distribution, as seen, e.g., in Taurus (Li & Hu 1998), Chamaeleon (Alcalá et al. 1997), and Lupus (Krautter et al. 1997).

It is known that different kinds of PMS stars, namely WTTSs, CTTSs, and HAeBe stars occupy different loci in the color-color diagram (Lada & Adams 1992). In particular, such a diagram is a useful tool to identify PMS stars with strong infrared excesses, i.e., HAeBe stars and CTTSs, or to distinct young stars from classical Be stars Hernández et al. (2005), which are evolved main-sequence early-type stars whose excess radiation is attributed mainly to free-free emission, rather than to dust thermal emission. In general, PMS stars associated with reflection nebulae or molecular outflows are redder than those without (Kenyon & Hartmann 1995). For example star groups associated with Perseus, Orion A, Orion B, and Monoceros R2 molecular clouds contains young stellar objects embedded in clouds Carpenter (2000).

Lee et al. (2005) use 2MASS color-color diagram to select CTTS candidates which lie

between the two parallel lines,  $(J-H) - 1.7(H-K_s) + 0.0976 = 0$  and  $(J-H) - 1.7(H-K) + 0.450 = 0$ , and above the dereddened CTTS locus (Meyer et al. 1997),  $(J-H) - 0.493(H-K_s) - 0.439 = 0$ . It has been known that HAeBe stars show more prominent infrared excesses than CTTSs (Lada & Adams 1992; Hernández et al. 2005). Therefore, Lee & Chen (2007) extend the selection criteria to include HAeBe stars with colors redder than the line,  $(J-H) - 1.7(H-K_s) + 0.450 = 0$ . Lee & Lim (2008) further improve the criteria for HAeBe candidates, resulting the region between the two parallel lines,  $(J-H) - 1.7(H-K_s) + 0.450 = 0$  and  $(J-H) - 1.7(H-K_s) + 1.400 = 0$ , and above the line  $(J-H) = 0.2$ , to be more discriminative to exclude contaminating sources such as B[e] and classical Be stars from the young star sample. The improved set of criteria has been used to study the star formation in Per OB1 at high Galactic latitudes (Lee & Lim 2008).

Figure 1 shows the overview of the Orion-Eridanus Superbubble in  $H\alpha$  (Finkbeiner 2003; Dennison et al. 1998; Gaustad et al. 2001; Haffner et al. 2003) and CO (Dame et al. 2001) images. All of the PMS candidate stars which were identified by 2MASS colors are plotted. A total of 692 CTTS and 198 HAeBe candidate stars have been identified in the region ( $\ell=175$  to  $230$  and  $b = -50$  to  $-5$ ). It is clear that the PMS candidate stars are concentrated in the Orion A and B giant molecular clouds. Because these PMS candidate stars are grouped or clustered together, they are likely to be PMS stars. On the other hand, some molecular clouds are associated with only a few PMS candidate stars. These candidates need spectroscopic observations to confirm their PMS nature.

## 2.2. Spectroscopic Observations

We took spectroscopic observations of bright PMS candidate stars in two regions, Region One ( $178^\circ < l < 188^\circ$ ,  $-32^\circ < b < -11^\circ$ ) and Region Two ( $215^\circ < l < 227^\circ$ ,  $-22^\circ < b < -8^\circ$ ). Region One includes the LDN 1551, LDN 1558, and LDN 1563 molecular clouds; Region Two includes NGC 2149, GN 05.51.4, VdB 64, and the Crossbones. Using the criteria described in §2.1, there are 21 CTTS and 13 HAeBe candidate stars in Region One, and 84 CTTS and 25 HAeBe candidates stars in Region Two.

The criteria of Lee & Chen (2007) were used to select PMS star sample in our first observing run at Kitt Peak National Observatory. Spectra of bright PMS stars in Region Two were taken with the 2.1 m telescope during 2004 January 1–5. The GoldCamera spectrometer, with a Ford  $3K \times 1K$  CCD with  $15 \mu\text{m}$  pixels, was used with the grating #26new, which gives a dispersion of  $1.24 \text{ \AA pixel}^{-1}$  and covers  $3800\text{--}7100 \text{ \AA}$ .

In the second observing run, at Beijing Astronomical Observatory, we used the modified

criteria (Lee & Lim 2008) to select our PMS candidate stars. For these, low-dispersion spectra with a dispersion of  $200 \text{ \AA mm}^{-1}$  (or  $4.8 \text{ \AA pixel}^{-1}$ ) were taken with the 2.16 m optical telescope during 2007 October 19–21. An OMR (Optomechanics Research, Inc.) spectrograph was used with a Princeton Instrument SPEC10 400×1300B CCD detector covering 3500–8500  $\text{\AA}$ . PMS candidate stars in both regions were included in the second run.

Spectra of lamp and standard stars were taken during both observing runs, and that would be used to perform wavelength and flux calibration. All the spectroscopic data were processed by the standard procedure with the NOAO/IRAF package. After correcting the bias and flat-fielding, the IRAF package KPNOSLIT was used to extract and to calibrate the wavelength and flux of each spectrum.

### 2.3. Results

In the two regions, we obtained spectra for a total of 43 bright PMS star candidates, with 12 stars in Region One and 31 in Region Two. Thirty two of these 43 candidates turn out to be bona fide PMS stars, with 10 HAeBe and 22 T Tauri stars, giving a success rate of about three quarters based on 2MASS colors.

Checking with SIMBAD<sup>1</sup>, we find 21 out of the 32 spectroscopically confirmed PMS stars new identifications. Table 1 lists the T Tauri, HAeBe stars, and non-PMS sources studied with our spectroscopic observations. We also determine, if applicable, the  $H\alpha$ , [O I], and [S II] equivalent widths of PMS stars. T Tauri stars with  $H\alpha$  equivalent widths greater than 10  $\text{\AA}$  are classified as CTTSs (Herbig & Bell 1988). In Table 1, stars 1–11 are located in Region One, and the others are in Region Two. Notably, there are HAeBe stars and CTTSs in Region Two, whereas only CTTSs are found in Region One, perhaps because of its smaller PMS sample. The spatial distribution of PMS stars in Table 1 is shown in Figure 2 and 3.

Originally, star 22 is classified as a K5 star with low-dispersion spectroscopy (Lee et al. 2005). We later realize, with higher dispersion and signal-to-noise ratio spectra, that it should be an F6 star. We also find that intermediate-mass PMS F-type stars, namely stars 22 and 37, do not show the lithium absorption line (6708  $\text{\AA}$ ) in their spectra.

---

<sup>1</sup><http://simbad.u-strasbg.fr/simbad/>

### 3. STAR FORMATION

Using near-infrared data, we can detect CTTSs with strong infrared excesses, but unavoidably will miss WTTSs or CTTSs with reduced infrared excesses. Although a complete census of young stellar objects is a crucial first step to study disk fraction evolution or the initial mass function, but it is not the purpose of this work. Instead, our goal is to trace *recent* star formation activity in clouds interacting with the Superbubble. Therefore, even if our PMS star sample may not be complete, it does not affect our results. Still, we include young stellar samples found in the literatures to supplement our sample.

Searching young stellar objects in SIMBAD including Variable Star of Orion Type (Or\*), T Tau-type Star (TT\*), Young Stellar Object (Y\*O), and Variable Star of FU Ori type (FU\*), we find 1647 objects in the same region that we search CTTSs and HAeBe stars from 2MASS. Figure 4 shows the distribution of the young stellar objects in SIMBAD. Most of the objects are distributed in Ori OB1, and clustered in LDN 1551. This means that previous studies concentrate on these regions. Compared with our sample, we do not find those young stellar objects away from molecular clouds, e.g., in Ori OB1a and 1b. These objects are mainly WTTSs (Briceño et al. 2001, 2005, 2007b), and that is why they are not selected by our criteria. We also miss a lot of young stellar objects in LDN 1551. On the other hand, our sample provides PMS star sample in the less explored regions, e.g., NGC 2149, VdB 64, and the Crossbones. We cross-correlate our PMS star sample and young stellar objects from SIMBAD for those young stars listed in the SIMBAD database for positional coincidence within  $5''$ , and find 86 CTTS and 20 HAeBe candidate stars in the region. Hereafter, we call the HAeBe star and CTTS candidates as HAeBe stars and CTTSs, respectively, for convenience.

#### 3.1. Orion A and B Giant Molecular Clouds

M42 is one of the most active nearby star-forming regions. Hillenbrand (1997) list nearly 1600 optically detected sources within 2.5 pc of the center. *Chandra* detects 1616 X-ray sources in the Orion Nebula (Getman et al. 2005; Feigelson et al. 2005). Compared to M42, NGC 2024 is more embedded, hence it requires X-ray or infrared observations to study the young stars in this region. *Chandra* detect 283 X-ray sources (Skinner et al. 2003), and Haisch et al. (2001a) find 257 sources in N band ( $10.8 \mu\text{m}$ ). M78 is less explored than previous two regions. There are only about six sources found in SIMBAD (Figure 4).

Megeath et al. (2005) use the *Spitzer* Space Telescope to survey the Orion A and B molecular clouds. Combined with the 2MASS data, they find more than one thousand

young stars, approximately half of which are grouped in clusters, e.g., NGC 2024 and the Orion Nebula, whereas the other half are distributed. These authors detect 487 sources in M 42, 239 in NGC 2024, and 229 in M 78. The limitation of the study by Megeath et al. (2005) is that they only survey the side of the Orion A molecular cloud with strong  $^{13}\text{CO}$  emission (Bally et al. 1987) and two fields of the Orion B cloud. In comparison, our study based on the 2MASS data does not find as many young stars as by Megeath et al. (2005), but our spatial coverage is much more extended in these two molecular clouds.

As seen in Figure 5, the intensity of the  $^{12}\text{CO}$  emission of the Orion A molecular cloud is distinctively stronger on one side, like a ridge separating Orion A into two parts. In Figure 5, the cloud as traced by  $^{13}\text{CO}$  emission shows filamentary structure, the most prominent being the integral-shaped filament including M 43 and M 42, which is thought to be the outcome of compression by the Superbubble (Bally et al. 1987). Most PMS stars are associated with  $^{13}\text{CO}$  emission, in particular with more than 150 PMS stars along the integral-shaped filament. The level of star-formation activity in Orion A increases from NGC 1977, peaks at M 43 and M 42, and then drops very quickly to the rest of the cloud.

The distribution of  $^{13}\text{CO}$  emission in the Orion B molecular cloud (Miesch & Bally 1994) is more conspicuous on the side facing Ori OB1a, where star formation is also more active (Figure 6). Star formation around Orion B is concentrated in three locations, M 78 (including the reflection nebulae M 78 and NGC 2071), NGC 2024, and the  $\sigma$  Ori cluster. We find some two dozen PMS stars in each of these locations.

As mentioned above, recent star formation primarily took place on the side facing Ori OB1a in both the Orion A and B clouds. Could there be nondetected CTTS (selected by near-infrared colors) embedded on the other side of the clouds? It is unlikely. The extinction of the regions not associated with CTTSs, as derived from the data in Froebrich et al. (2007), is generally low, mostly with  $A_J \lesssim 0.6$  mag, so any CTTSs, if they exist, could not have escaped from the detection by 2MASS. In comparison, the extinction of star-forming clouds in Orion A and B is typically  $A_J > 0.8$  mag or much higher. Our PMS sample, naturally limited by the 2MASS sensitivity, thus should be substantially complete for CTTSs showing large near-infrared excess. It is therefore a secured conclusion that CTTSs with strong infrared excesses are distributed predominantly on the side facing Ori OB1a.

### 3.2. NGC 2149, GN 05.51.4, VdB 64, and the Crossbones

Relative to other star-forming regions in Orion A and B, NGC 2149, GN 05.51.4, VdB 64, and the Crossbones are not as explored. They have been mapped in  $^{12}\text{CO}$  (Wilson et al. 2005;



Maddalena et al. 1986) and  $^{13}\text{CO}$  (Kim et al. 2004). Figure 3 depicts the  $\text{H}\alpha$  (Finkbeiner 2003) and extinction maps (Froebrich et al. 2007) of this region. The CO radial velocities of NGC 2149, GN 05.51.4 and VdB 64 (Wilson et al. 2005; Kim et al. 2004) are similar to that of Ori A, with  $\sim 10\text{--}12 \text{ km s}^{-1}$ , so a distance of 425 pc is adopted for these clouds. We find 12 PMS candidates in NGC 2149, 5 in GN 05.51.4, and 7 in VdB 64. Of these, 7 in NGC 2149, 2 in GN 05.51.4, and 4 in VdB 64 are spectroscopically confirmed to be bona fide T Tauri stars (Table 1).

The elongated Crossbones cloud includes the reflection nebula VdB 80 and the dark cloud LDN 1652. There are 42 PMS stars found in the Crossbones (Fig. 1 and 3). Interestingly, these young stars are not centrally concentrated as in a star cluster, but rather are distributed along the elongated cloud. Stars 39, 40, 42, and 43 in Table 1 and stars 20 – 24 in Lee et al. (2005) are associated with the Crossbones, the majority (7 out of 9) of which exhibit forbidden line(s), indicative of youth (Kenyon et al. 1998). Besides CTTs, there is an HAeBe star, PDS 23 (Vieira et al. 2003; Gregorio-Hetem et al. 1992), in this cloud.

### 3.3. Northern Filament

The Northern Filament is a long, narrow cloud, with an estimated mass of  $1.7 \times 10^4 M_{\odot}$  (Wilson et al. 2005). It is located near the Orion B molecular cloud, but closer to the Galactic plane (Figure 1). Without knowledge of possible stars associated with the cloud, the distance of the Northern Filament can only be inferred by indirect methods. Maddalena et al. (1986) estimate a distance of  $800 \pm 170 \text{ pc}$  from star counts, but adopt a distance of 500 pc in view of its similar radial velocity as the nearby Orion B cloud, which is at a distance of 500 pc. Recently, Wilson et al. (2005) use foreground and background stars from *Hipparcos* catalogue to determine a distance of  $393_{-48}^{+65}$ .

There is no sign of ongoing star formation in the Northern Filament (Maddalena et al. 1986)—no H II region or reflection nebula—and indeed we find no apparent PMS star groups in the Northern Filament, despite the expectation of some hundreds of young stars in the region (Wilson et al. 2005). This cloud thus serves as a good comparison case in an otherwise active star-forming region.

### 3.4. LDN 1551, LDN 1558, and LDN 1563

The clouds LDN 1551, LDN 1558, and LDN 1563 are located on the periphery of the Superbubble, outlined by  $\text{H}\alpha$  filaments. LDN 1551 offers one of the best examples of a

superbubble-cloud interaction. In Figure 1 and 2, the  $H\alpha$  filament follows the rim of the comet-shaped cloud. Moriarty-Schieven et al. (2006) find that the cloud points to the direction of Orion, and argue that the outline of LDN 1551 is illuminated and eroded by Ori OB1.

There are at least 30 PMS stars in LDN 1551 (Luhman 2006; Gomez et al. 1993; Briceño et al. 1998; Moriarty-Schieven et al. 2006). Multi-generational star formation in LDN 1551 is suggested by Moriarty-Schieven et al. (2006), spanning the past few million years and leading to the formation of two small clusters of protostars, together with a halo of more evolved PMS stars. Note that almost all PMS stars are located near the rim of the cloud, whereas protostars are embedded inside the cloud. The distribution of PMS stars is similar to what is seen in the bright-rimmed clouds in Ori OB1 and Lac OB1 (Lee et al. 2005; Lee & Chen 2007; Chen et al. 2007; Chen & Lee 2008), implying sequential star formation in LDN 1551.

Star 9 in our list (DR Tau), with a distance of  $138_{-37}^{+82}$  pc (Bertout & Genova 2006), is likely associated with LDN 1558 (see Fig. 2). Additional young stellar objects around LDN 1558 include the CTTSs, DQ Tau and Haro 6–37 (Furlan et al. 2005). According to the UCAC2 catalog (Zacharias et al. 2004), the proper motion of DQ Tau is  $(4.2 \pm 6.0 \text{ mas yr}^{-1}, -24.6 \pm 5.9 \text{ mas yr}^{-1})$ , similar to that of DR Tau  $(5.2 \pm 6.2 \text{ mas yr}^{-1}, -26.8 \pm 5.4 \text{ mas yr}^{-1})$ . On the other hand, the proper motion of Haro 6–37  $(-19.1 \pm 6.0 \text{ mas yr}^{-1}, -57.1 \pm 6.0 \text{ mas yr}^{-1})$  is very different. We assume that the LDN 1558 molecular cloud is the birthplace for DR Tau and DQ Tau, so a distance of 138 pc is adopted for LDN 1558.

LDN 1563 is associated with Sh 2–246, a nebula with  $H\alpha$  emission (Fich et al. 1990). There are no O or early B stars close to LDN 1563, so the  $H\alpha$  emission likely arises from the Superbubble. In addition, the morphology of LDN 1563 is similar to that of LDN 1551, both appearing comet-shaped pointing to the direction of Ori OB1. Star 10 is projected close to, so is likely related to, LDN 1563.

## 4. DISCUSSION

### 4.1. Structure of the Superbubble

It is hard to know the real three-dimensional structure of the Superbubble, because the distance to each edge is uncertain. Burrows et al. (1993) generate a model for the Superbubble, based on what was proposed by Reynolds & Ogden (1979), with the boundary of the Superbubble estimated only circumstantially. Since Ori OB1 is responsible for ionization of the Superbubble (Reynolds & Ogden 1979), those clouds within or on the border of the

Superbubble should exhibit  $H\alpha$  emission. We sketch the structure of the Superbubble in Figure 7, in relation with the molecular clouds and the OB subgroups in Ori OB1. In addition to the molecular clouds discussed in §3, we also include here three molecular clouds, IC 2118 (Kun et al. 2001, 2004), LDN 1616 (Alcalá et al. 2004; Gandolfi et al. 2008), and LDN 1634 (Stephenson 1986; Downes & Keyes 1988), which have been studied in our previous papers to be outlined also by  $H\alpha$  filaments (Lee et al. 2005; Lee & Chen 2007).

Compared with previous works of Reynolds & Ogden (1979) and of Burrows et al. (1993), our Superbubble model extends further to the Galactic plane, as delineated by the  $H\alpha$  emission (Figure 1), with Ori OB1a located roughly at the center. Table 2 lists the distance to each cloud from us, and the distance between the cloud and the center of the Superbubble, i.e., Ori OB1a. The relative position of each cloud is shown in Figure 7, where one sees a distribution of  $H\alpha$  clouds along the border of the Superbubble. This kind of phenomenon has been known in other superbubbles, e.g., the Cepheus ring (Kun et al. 1987; Balazs & Kun 1989), the Per OB1 superbubble (Lee & Lim 2008), the Carina flare (Fukui et al. 1999; Dawson et al. 2008), and the H I loop related to NGC 281 (Sato et al. 2007).

LDN 1551, LDN 1558, and LDN 1563 reside at the near edge of the Superbubble, about 140–180 pc away from us. This is consistent with the 21 cm and Na D observations by Guo et al. (1995), who estimate the distance to the near side of the Superbubble to be  $159 \pm 16$  pc. As seen in Figure 7, the Northern Filament is located outside the Superbubble. This explains why it is not associated with  $H\alpha$  filament or any star formation.

## 4.2. Triggered Star Formation

As discussed in §3, clouds coincident with  $H\alpha$  filaments are associated with star formation. A superbubble may play an important role in sequential star formation in an OB association (see, e.g., the reviews by Tenorio-Tagle & Bodenheimer 1988; Elmegreen 1998). In the Orion A and B molecular clouds that we investigate, PMS stars correlate well with filamentary structures (§3.1), which were caused by the massive stars in Ori OB1 (Bally et al. 1991). That young stars are closely associated with filaments provides strong evidence of triggered star formation, in that massive stars cause clouds to be swept up to high density, i.e., filamentary structures, and then stars form in the compressed regions.

Brown et al. (1994) propose a star formation sequence in the Ori OB1 association; namely it started from subgroup Ori OB1a, and propagated to subgroups 1b, 1c, and eventually to 1d. Our study extends the diagnosis of the star formation history to the border of the

Superbubble (Figure 8), which was created by the stellar winds and supernova explosions of the luminous stars in Ori OB1. The Superbubble expanded and interacted with clouds such as the Crossbones, NGC 2149, GN 05.51.4, and VdB 64. The Crossbones is well outlined by H $\alpha$  filaments, which is manifest of interaction (Figure 3). The correlation between the compressed high-density gas and existence of young stars in the Crossbones accordingly provides a vivid example of star formation triggered by the Superbubble. NGC 2149, GN 05.51.4 and VdB 64 are seen also associated with H $\alpha$  filaments (Figure 3), though not as clear as the Crossbones. On the opposite side, the Superbubble appears to have interacted with and prompted star formation in LDN 1551, LDN 1563, and LDN 1558 as well (Figure 2).

Briceño et al. (2007a) claim that shock velocities in the range of 15–45 km s<sup>-1</sup> are able to induce star formation in molecular cores. Velocities faster than 45 km s<sup>-1</sup> would shred cloud cores to pieces whereas velocities slower than 15 km s<sup>-1</sup> would be unable to trigger a core to collapse. The expansion velocity of the Orion-Eridanus Superbubble is measured to be  $\sim 15$  km s<sup>-1</sup> (Reynolds & Ogden 1979), marginally high enough to play a constructive role in induced star formation. It appears that the Northern Filament provides a case for a cloud neither reaching the critical density to collapse spontaneously, nor being compressed by the Superbubble.

Given the distance ( $D$ ) between a cloud and Ori OB1a (see Table 2), and the expansion velocity ( $V$ ) of the Superbubble, the dynamical timescale ( $t$ ) of the Superbubble can be estimated by  $t \simeq \eta D V^{-1}$  (Book et al. 2008), where  $\eta$  is 0.6 for an energy-conserved bubble (Castor et al. 1975; Weaver et al. 1977) and 0.4 for a momentum-conserved bubble (Steigman et al. 1975). Here, we adopt an average value  $\eta=0.5$  to derive a dynamical timescale  $t$  to be in the range of 4.3–8.8 Myr for the near and far edges of the Superbubble.

In a triggered star-formation scenario, the age of an O star, if it is still in existence, must be at least comparable to the ages of next-generation young stars plus the shock traveling time of a superbubble. In our case, the Superbubble was created by the massive stars in Ori OB1a, whose main-sequence lifetimes are some 11 Myr (Brown et al. 1994). Because a typical CTTS would lose its disk in 6 Myr (Haisch et al. 2001b), the CTTSs that we have found, all with ample NIR excesses, should be no more than a few million years old. Therefore, the causality holds to support a triggered star formation process in terms of the ages of Ori OB1a (11.4 Myr), the transverse time of Superbubble (4.3–8.8 Myr), and typical ages of CTTSs ( $\lesssim 6$  Myr).

## 5. CONCLUSIONS

We have conducted a census of classical T Tauri and Herbig Ae/Be stars selected by 2MASS colors in the vicinity of the Orion-Eridanus Superbubble produced by Ori OB1. Our study results in young star samples in two giant molecular clouds (Orion A and B) and additional smaller molecular clouds, including NGC 2149, GN 05.51.4, VdB 64, the Crossbones, the Northern Filament, LDN 1551, LDN 1558, and LDN 1563. Combined with  $H\alpha$  and CO images, we investigate the star formation history in this region. The main results of our work are summarized as follows:

1. Clouds associated with  $H\alpha$  filaments are preferentially located on the border of the Orion-Eridanus Superbubble, created by UV photons from luminous stars in Ori OB1. Clouds outlined by  $H\alpha$  filaments exhibit recent star formation.
2. The Northern Filament neither accompanies  $H\alpha$  filament, nor is associated with PMS stars. It is likely to be situated outside, hence out of reach of the compression by, the Superbubble to form stars.
3. Star formation triggered by the expanding Orion-Eridanus Superbubble started from Ori OB1a and propagated to other subgroups. The Superbubble not only triggered starbirth in Orion A and B, but also led to current star formation in NGC 2149, GN 05.51.4, VdB 64, and the Crossbones which are located some one hundred pc away from Ori OB1a.
4. The Superbubble likely also prompted star formation in clouds some two hundred pc away from Ori OB1a, as witnessed in LDN 1551, LDN 1563, and LDN 1558.
5. The triggered star formation scenario is supported by sequential star formation, ages of PMS stars in the clouds, and the expansion timescale of the Superbubble.

We thank the anonymous referee for detailed reading, constructive comments, and suggestions. We want to thank specially Richard F. Green who kindly provided us KPNO director's discretionary time for this study. Our gratitude goes to John Bally for providing  $^{13}\text{CO}$  maps of Ori A and Ori B and to You-Hua Chu for helpful discussions. We thank Jinzeng Li and the staff at the Beijing Astronomical Observatory for their assistance during our observing runs. This research makes use of data from the Two Micron All Sky Survey (2MASS) and the Southern H-Alpha Sky Survey Atlas (SHASSA). We acknowledge the financial support of the grants NSC95-2119-M-008-028 and NSC95-2745-M-008-002 of the National Science Council of Taiwan.

## REFERENCES

- Alcalá, J. M., et al. 1996, *A&AS*, 119, 7
- Alcalá, J. M., Krautter, J., Covino, E., Neuhaeuser, R., Schmitt, J. H. M. M., & Wichmann, R. 1997, *A&A*, 319, 184
- Alcalá, J. M., Chavarria-K., C., & Terranegra, L. 1998, *A&A*, 330, 1017
- Alcalá, J. M., Covino, E., Torres, G., Sterzik, M. F., Pfeiffer, M. J., & Neuhäuser, R. 2000, *A&A*, 353, 186
- Alcalá, J. M., Wachter, S., Covino, E., Sterzik, M. F., Durisen, R. H., Freyberg, M. J., Hoard, D. W., & Cooksey, K. 2004, *A&A*, 416, 677
- Balazs, L. G., & Kun, M. 1989, *Astronomische Nachrichten*, 310, 385
- Bally, J., Stark, A. A., Wilson, R. W., & Langer, W. D. 1987, *ApJ*, 312, L45
- Bally, J., Langer, W. D., Wilson, R. W., Stark, A. A., & Pound, M. W. 1991, in *IAU Symp. 147: Fragmentation of Molecular Clouds and Star Formation*, ed. E. Falgarone, F. Boulanger, & G. Duvert (Dordrecht: Kluwer), 11
- Bertout, C., Robichon, N., & Arenou, F. 1999, *A&A*, 352, 574
- Bertout, C., & Genova, F. 2006, *A&A*, 460, 499
- Blaauw, A. 1991, in *The Physics of Star Formation and Early Stellar Evolution*, ed. C J. Lada & N. D. Kylafis (NATO ASI Ser. C, 342; Dordrecht: Kluwer), 125
- Blaauw, A. 1964, *ARA&A*, 2, 213
- Book, L. G., Chu, Y.-H., & Gruendl, R. A. 2008, *ApJS*, 175, 165
- Briceño, C., Preibisch, T., Sherry, W. H., Mamajek, E. A., Mathieu, R. D., Walter, F. M., & Zinnecker, H. 2007, *Protostars and Planets V*, 345
- Briceño, C., Hartmann, L., Hernández, J., Calvet, N., Vivas, A. K., Furesz, G., & Szentgyorgyi, A. 2007, *ApJ*, 661, 1119
- Briceño, C., Calvet, N., Hernández, J., Vivas, A. K., Hartmann, L., Downes, J. J., & Berlind, P. 2005, *AJ*, 129, 907
- Briceño, C., et al. 2001, *Science*, 291, 93

- Briceño, C., Hartmann, L., Stauffer, J., & Martín, E. 1998, *AJ*, 115, 2074
- Brown, A. G. A., de Geus, E. J., & de Zeeuw, P. T. 1994, *A&A*, 289, 101
- Brown, A. G. A., Hartmann, D., & Burton, W. B. 1995, *A&A*, 300, 903
- Burrows, D. N., Singh, K. P., Nousek, J. A., Garmire, G. P., & Good, J. 1993, *ApJ*, 406, 97
- Carpenter, J. M., Hillenbrand, L. A., & Skrutskie, M. F. 2001, *AJ*, 121, 3160
- Carpenter, J. M. 2000, *AJ*, 120, 3139
- Castor, J., McCray, R., & Weaver, R. 1975, *ApJ*, 200, L107
- Chen, W. P., Lee, H.-T., & Sanchawala, K. 2007, in “Triggered Star Formation in a Turbulent ISM”, Ed. B. G. Elmegreen & J. Palous, *IAUS*, 237, 278
- Chen, W. P., & Lee, H.-T. in “Handbook of Star Forming Regions”, Ed. Bo Reipurth, *ASPC* (in press)
- Clark, F. O., Laureijs, R. J., & Wardell, L. L. 1991, *ApJ*, 370, 237
- Cutri, R. M., et al. 2003, *2MASS All Sky Catalog of Point Sources* (Pasadena:IPAC)
- Dame, T. M., Hartmann, D., & Thaddeus, P. 2001, *ApJ*, 547, 792
- Dawson, J. R., Mizuno, N., Onishi, T., McClure-Griffiths, N. M., & Fukui, Y. 2008, *MNRAS*, 387, 31
- Dennison, B., Simonetti, J. H., & Topasna, G. A. 1998, *Publications of the Astronomical Society of Australia*, 15, 147
- de Zeeuw, P. T., Hoogerwerf, R., de Bruijne, J. H. J., Brown, A. G. A., & Blaauw, A. 1999, *AJ*, 117, 354
- Downes, R. A., & Keyes, C. D. 1988, *AJ*, 96, 777
- Elmegreen, B. G. 1998, *ASP Conf. Ser.* 148: *Origins*, 150
- Feigelson, E. D., et al. 2005, *ApJS*, 160, 379
- Feigelson, E. D., & Montmerle, T. 1999, *ARA&A*, 37, 363
- Fich, M., Dahl, G. P., & Treffers, R. R. 1990, *AJ*, 99, 622
- Finkbeiner, D. P. 2003, *ApJS*, 146, 407

- Froebrich, D., Murphy, G. C., Smith, M. D., Walsh, J., & Del Burgo, C. 2007, *MNRAS*, 378, 1447
- Fukui, Y., Onishi, T., Abe, R., Kawamura, A., Tachihara, K., Yamaguchi, R., Mizuno, A., & Ogawa, H. 1999, *PASJ*, 51, 751
- Furlan, E., et al. 2005, *ApJ*, 628, L65
- Gandolfi, D., et al. 2008, *ArXiv e-prints*, 807, arXiv:0807.0532
- Gaustad, J. E., McCullough, P. R., Rosing, W., & Van Buren, D. 2001, *PASP*, 113, 1326
- Getman, K. V., et al. 2005, *ApJS*, 160, 319
- Gomez, M., Hartmann, L., Kenyon, S. J., & Hewett, R. 1993, *AJ*, 105, 1927
- Gregorio-Hetem, J., Lepine, J. R. D., Quast, G. R., Torres, C. A. O., & de La Reza, R. 1992, *AJ*, 103, 549
- Guo, Z., Burrows, D. N., Sanders, W. T., Snowden, S. L., & Penprase, B. E. 1995, *ApJ*, 453, 256
- Haisch, K. E., Jr., Lada, E. A., Piña, R. K., Telesco, C. M., & Lada, C. J. 2001, *AJ*, 121, 1512
- Haisch, K. E., Jr., Lada, E. A., & Lada, C. J. 2001, *ApJ*, 553, L153
- Haffner, L. M., Reynolds, R. J., Tufte, S. L., Madsen, G. J., Jaehnig, K. P., & Percival, J. W. 2003, *ApJS*, 149, 405
- Heiles, C. 1976, *ApJ*, 208, L137
- Heiles, C., Haffner, L. M., & Reynolds, R. J. 1999, in *ASP Conf. Ser. 168, New Perspectives on the Interstellar Medium*, ed. A. R. Taylor, T. L. Landecker, & G. Joncas (San Francisco: ASP), 211
- Herbig, G. H. & Bell, K. R. 1988, *Third Catalog of Emission-Line Stars of the Orion Population* (Lick Obs. Bull. 1111; Santa Cruz: Lick Obs.)
- Herbst, W., Herbst, D. K., Grossman, E. J., & Weinstein, D. 1994, *AJ*, 108, 1906
- Hernández, J., et al. 2007, *ApJ*, 671, 1784
- Hernández, J., et al. 2007, *ApJ*, 662, 1067



- Hernández, J., Calvet, N., Hartmann, L., Briceño, C., Sicilia-Aguilar, A., & Berlind, P. 2005, *AJ*, 129, 856
- Hernández, J., Calvet, N., Briceño, C., Hartmann, L., & Berlind, P. 2004, *AJ*, 127, 1682
- Hillenbrand, L. A. 1997, *AJ*, 113, 1733
- Humphreys, R. M. 1978, *ApJS*, 38, 309
- Kenyon, S. J., Brown, D. I., Tout, C. A., & Berlind, P. 1998, *AJ*, 115, 2491
- Kenyon, S. J., & Hartmann, L. 1995, *ApJS*, 101, 117
- Krautter, J., Wichmann, R., Schmitt, J. H. M. M., Alcalá, J. M., Neuhauser, R., & Terrane-gra, L. 1997, *A&AS*, 123, 329
- Kim, B. G., Kawamura, A., Yonekura, Y., & Fukui, Y. 2004, *PASJ*, 56, 313
- Kogure, T., Yoshida, S., Wiramihardja, S. D., Nakano, M., Iwata, T., & Ogura, K. 1989, *PASJ*, 41, 1195
- Kun, M., Balazs, L. G., & Toth, I. 1987, *Ap&SS*, 134, 211
- Kun, M., Aoyama, H., Yoshikawa, N., Kawamura, A., Yonekura, Y., Onishi, T., & Fukui, Y. 2001, *PASJ*, 53, 1063
- Kun, M., Prusti, T., Nikolić, S., Johansson, L. E. B., & Walton, N. A. 2004, *A&A*, 418, 89
- Lada, C. J., & Adams, F. C. 1992, *ApJ*, 393, 278
- Lada, E. A., Evans, N. J., II, Depoy, D. L., & Gatley, I. 1991, *ApJ*, 371, 171
- Lee, H.-T., & Lim, J. 2008, *ApJ*, 679, 1352
- Lee, H.-T., & Chen, W. P. 2007, *ApJ*, 657, 884
- Lee, H.-T., Chen, W. P., Zhang, Z., & Hu, J. 2005, *ApJ*, 624, 808
- Li, J. Z., & Hu, J. Y. 1998, *A&AS*, 132, 173
- Luhman, K. L. 2006, *ApJ*, 645, 676
- Maddalena, R. J., Moscowitz, J., Thaddeus, P., & Morris, M. 1986, *ApJ*, 303, 375
- Megeath, S. T., et al. 2005, *IAU Symposium*, 227, ed. Cesaroni, R., Felli, M., Churchwell, E., & Walmsley, M. (Cambridge: Cambridge University Press), 383

- Meyer, M. R., Calvet, N., & Hillenbrand, L. A. 1997, *AJ*, 114, 288
- Miesch, M. S., & Bally, J. 1994, *ApJ*, 429, 645
- Moriarty-Schieven, G. H., Johnstone, D., Bally, J., & Jenness, T. 2006, *ApJ*, 645, 357
- Neuhäuser, R., Sterzik, M. F., Torres, G., & Martin, E. L. 1995, *A&A*, 299, L13
- Neuhäuser, R., et al. 2000, *A&AS*, 146, 323
- Parizot, E. M. G. 1998, *A&A*, 331, 726
- Reynolds, R. J., & Ogden, P. M. 1979, *ApJ*, 229, 942
- Sato, M., et al. 2007, *PASJ*, 59, 743
- Sivan, J. P. 1974, *A&AS*, 16, 163
- Skinner, S., Gagné, M., & Belzer, E. 2003, *ApJ*, 598, 375
- Snowden, S. L., Burrows, D. N., Sanders, W. T., Aschenbach, B., & Pfeffermann, E. 1995, *ApJ*, 439, 399
- Steigman, G., Strittmatter, P. A., & Williams, R. E. 1975, *ApJ*, 198, 575
- Stephenson, C. B. 1986, *ApJ*, 300, 779
- Sterzik, M. F., Alcalá, J. M., Neuhaeuser, R., & Schmitt, J. H. M. M. 1995, *A&A*, 297, 418
- Tenorio-Tagle, G., & Bodenheimer, P. 1988, *ARA&A*, 26, 145
- Ungerechts, H., & Thaddeus, P. 1987, *ApJS*, 63, 645
- Vieira, S. L. A., Corradi, W. J. B., Alencar, S. H. P., Mendes, L. T. S., Torres, C. A. O., Quast, G. R., Guimarães, M. M., & da Silva, L. 2003, *AJ*, 126, 2971
- Walter, F. M., Alcalá, J. M., Neuhauser, R., Sterzik, M., & Wolk, S. J. 2000, *Protostars and Planets IV*, ed. V. Mannings, A. P. Boss, & S. S. Russell (Tucson: Univ. Arizona Press), 273
- Warren, W. H., & Hesser, J. E. 1978, *ApJS*, 36, 497
- Weaver, R., McCray, R., Castor, J., Shapiro, P., & Moore, R. 1977, *ApJ*, 218, 377
- Wichmann, R., et al. 1996, *A&A*, 312, 439

- Wichmann, R., Krautter, J., Covino, E., Alcalá, J. M., Neuhaeuser, R., & Schmitt, J. H. M. M. 1997, *A&A*, 320, 185
- Wilson, B. A., Dame, T. M., Masheded, M. R. W., & Thaddeus, P. 2005, *A&A*, 430, 523
- Wiramihardja, S. D., Kogure, T., Yoshida, S., Ogura, K., & Nakano, M. 1989, *PASJ*, 41, 155
- Wiramihardja, S. D., Kogure, T., Yoshida, S., Nakano, M., Ogura, K., & Iwata, T. 1991, *PASJ*, 43, 27
- Wiramihardja, S. D., Kogure, T., Yoshida, S., Ogura, K., & Nakano, M. 1993, *PASJ*, 45, 643
- Zacharias, N., Urban, S. E., Zacharias, M. I., Wycoff, G. L., Hall, D. M., Monet, D. G., & Rafferty, T. J. 2004, *AJ*, 127, 3043

Table 1. Spectral Observations

Star	2MASS	Emission Line(s) <sup>a</sup>	Li <sup>b</sup>	Type	Remarks
01	J03595596+0919044		-	C	
02	J04191911+1427140		-	C	
03	J04254487+1610141		-	C	C* 3243
04	J04314007+1813571	H(-71.5), O(-3.7), S(-3.7), Ca, Fe, He	-	CTTS	XZ Tau, associated with LDN 1551
05	J04360131+1726120	H(-30.8)	-	CTTS <sup>d</sup>	
06	J04442877+1221118		-	AGN	LEDA 2816425
07	J04462180+1723031		-	C	V1027 Tau
08	J04464456+1837505		-	M	
09	J04470620+1658428	H(-66.7), Ca, Fe, He	-	CTTS	DR Tau, associated with LDN 1558
10	J05001726+1348576	H(-37.7), O(-4.0), Ca	-	CTTS <sup>d</sup>	close to LDN 1563
11	J05045222+2210340		-	C	IRAS 05018+2206
12	J05534559-1024510	H(-203.3), Ca	-	CTTS <sup>d</sup>	associated with GN 05.51.4
13	J05550798-2113049		-	AGN	z=0.285
14	J05534254-1024006	H(-43.4), O(-1.3), S(-0.3)	n	HAeBe(B7)	IRAS 05513-1024, associated with GN 05.51.4
15	J05595090-0952488	H(-145.2), O(-1.7), Fe, He, Na	a	CTTS <sup>d</sup>	IRAS F05574-0952
16	J05561496-1221599	H(-6.0)	-	WTTS <sup>d</sup>	
17	J05574918-1406080	H <sup>c</sup>	-	HAeBe <sup>d</sup>	associated with VdB 64
18	J05574947-1405336	H <sup>c</sup>	-	HAeBe	IRAS 05555-1405, associated with VdB 64
19	J05580493-1332592	H(-33.3)	-	CTTS <sup>d</sup>	
20	J05585792-1327412	H(-33.1)	-	CTTS <sup>d</sup>	
21	J06003451-0953341	H(-114.6)	-	CTTS <sup>d</sup>	
22	J06014515-1413337	H(-4.4)	n	HAeBe(F6)	IRAS 05594-1413, (LCZ2005) 13
23	J06021488-1000595	H(-75.1), Fe	n	HAeBe(B4)	V791 Mon, IRAS 05598-1000
24	J06023181-0946510	H(-22.8)	n	CTTS <sup>d</sup>	
25	J06031315-0859167	H(-15.3)	-	CTTS <sup>d</sup>	
26	J06032324-0944118	H(-357)	-	CTTS <sup>d</sup>	associated with NGC 2149
27	J06032727-0941271	H(-100.4), Ca	-	CTTS <sup>d</sup>	associated with NGC 2149

Table 1—Continued

Star	2MASS	Emission Line(s) <sup>a</sup>	Li <sup>b</sup>	Type	Remarks
28	J06033705-1453025	H(-15.8)	n	HAeBe(B6)	AE Lep, IRAS 06013-1452
29	J06041782-1003349	H(-8.5)	n	HAeBe(B7) <sup>d</sup>	IRAS 06019-1003
30	J06063868-1544195	H(-16.7)	-	CTTS <sup>d</sup>	close to GN 06.03.6
31	J06072583-0831044	H(-7.3)	n	HAeBe(A9) <sup>d</sup>	IRAS 06050-0830
32	J06090348-1735089		n	AGN	z=0.104
33	J06091346-1011386	H(-22.1)	-	CTTS <sup>d</sup>	
34	J06092371-1009549	H(-31.5)	-	CTTS <sup>d</sup>	
35	J06092550-0938492	H(-142.9), O(-3.3), Fe	a	CTTS	AS 119, IRAS 06070-0938
36	J06160006-1727270		n	C	(LCZ2005) 29
37	J06181637-1702347	H <sup>c</sup>	n	HAeBe(F8)	UY CMa
38	J06205595-0754362	H(-21.3)	n	HAeBe(A4) <sup>d</sup>	
39	J06265390-1015349	H(-48.3), O(-3.8), He, Fe	n	CTTS	NSV 2968, associated with Crossbones
40	J06273428-1002397	H(-1.8)	a	WTTS	(LCZ2005) 23, associated with Crossbones
41	J06281742-1303109	H(-179.3), O(-2.7), Fe	n	B[e]	with [Fe II] line emission, HD 45677
42	J06294017-0953463	H(-6.2), O(-0.6)	a	CTTS <sup>d</sup>	IRAS 06272-0951, associated with Crossbones
43	J06312038-0927047	H(-131.1), O(-4.3), Fe, He	a	CTTS <sup>d</sup>	IRAS 06289-0924, associated with Crossbones

<sup>a</sup>H–H $\alpha$ , O–[O I], S–[S II], He–He I(6678), Fe–Fe, Ca–Ca II, Na–Na I, The number following H, O, S, are the equivalent widths of H $\alpha$ , [O I], and [S II], respectively.

<sup>b</sup>- low resolution spectrum; n – no detection; a – absorption

<sup>c</sup>Hydrogen Balmer lines are in absorption but filled in by H $\alpha$  emission.

<sup>d</sup>New identified PMS star.

Table 2. Distances of Clouds

Region	Heliocentric distance (pc)	Distance to Ori OB1a (pc)	Reference	Star Formation
LDN 1551	139	212	Bertout et al. (1999)	T Tau stars only
LDN 1558	138	209	Bertout & Genova (2006)	T Tau stars only
LDN 1563	180	264	Clark et al. (1991)	T Tau stars only
NGC 2149	425	134	Wilson et al. (2005)	H AeBe stars and CTTSs
GN 05.51.4	425 <sup>a</sup>	129	Wilson et al. (2005); Kim et al. (2004)	H AeBe star and CTTS
VdB 64	425	148	Wilson et al. (2005)	H AeBe stars and CTTSs
Crossbones	457	184	Wilson et al. (2005)	H AeBe stars and CTTSs

<sup>a</sup>The CO radial velocity of GN 05.51.4 (Kim et al. 2004) is similar to NGC 2149, so we assume that the distances of GN 05.51.4 and NGC 2149 are the same.

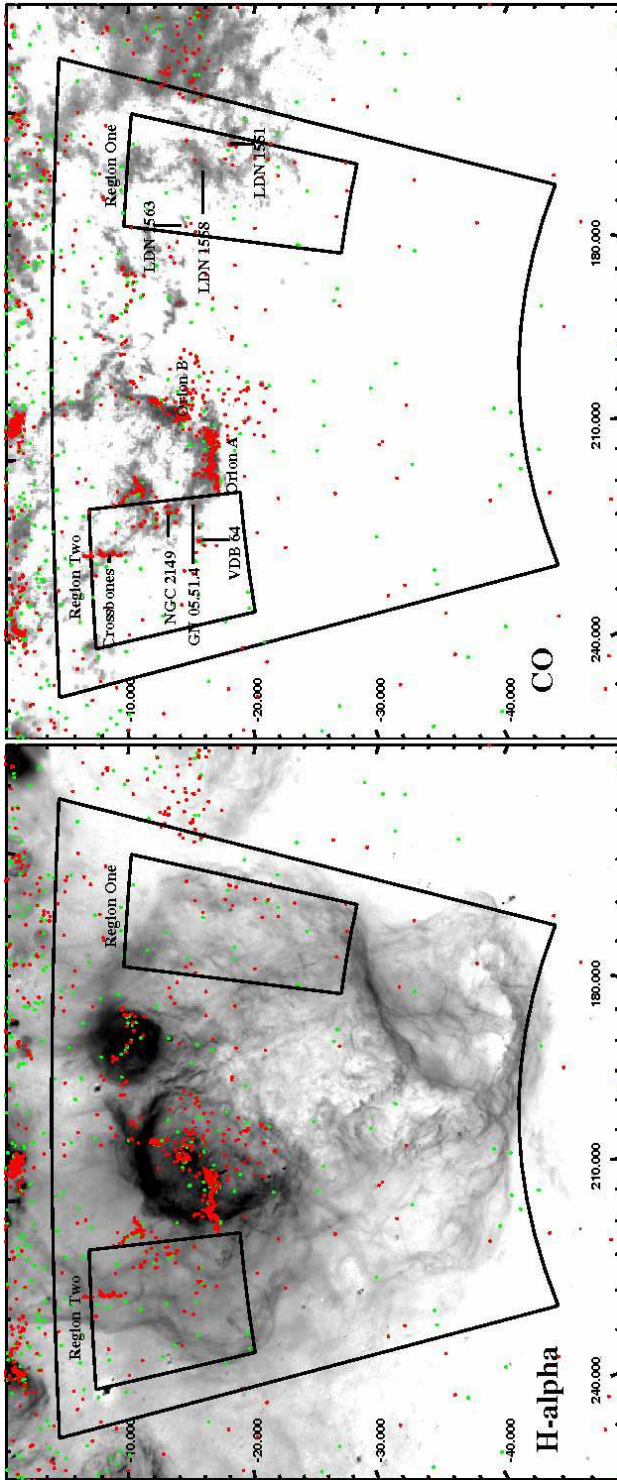


Fig. 1.—  $H\alpha$  (Finkbeiner 2003) and  $^{12}\text{CO}$  (Dame et al. 2001) images of the Orion-Eridanus Superbubble in Galactic coordinates. The red and green dots are CTTSs and HAeBe candidate stars, respectively, which are selected by their near-infrared colors. Solid lines indicate the region studying in this paper.

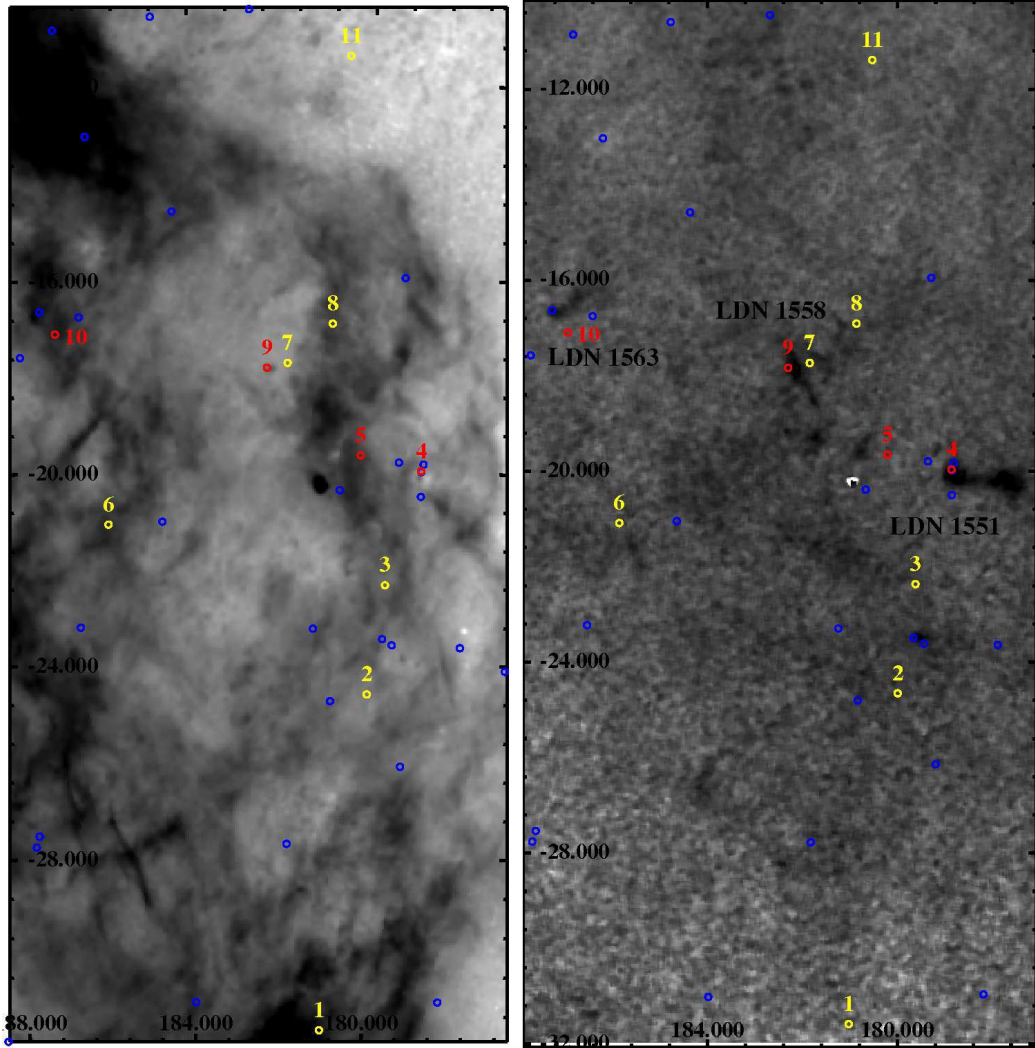


Fig. 2.—  $H\alpha$  image (left, (Finkbeiner 2003)) and extinction map (right, (Froebrich et al. 2007)) around the Region One. Stars with spectra type in Table 1 are labeled. The red, green, yellow, and blue circles are CTTSs, HAeBe, non-PMS, and PMS candidate stars selected by 2MASS colors, respectively.



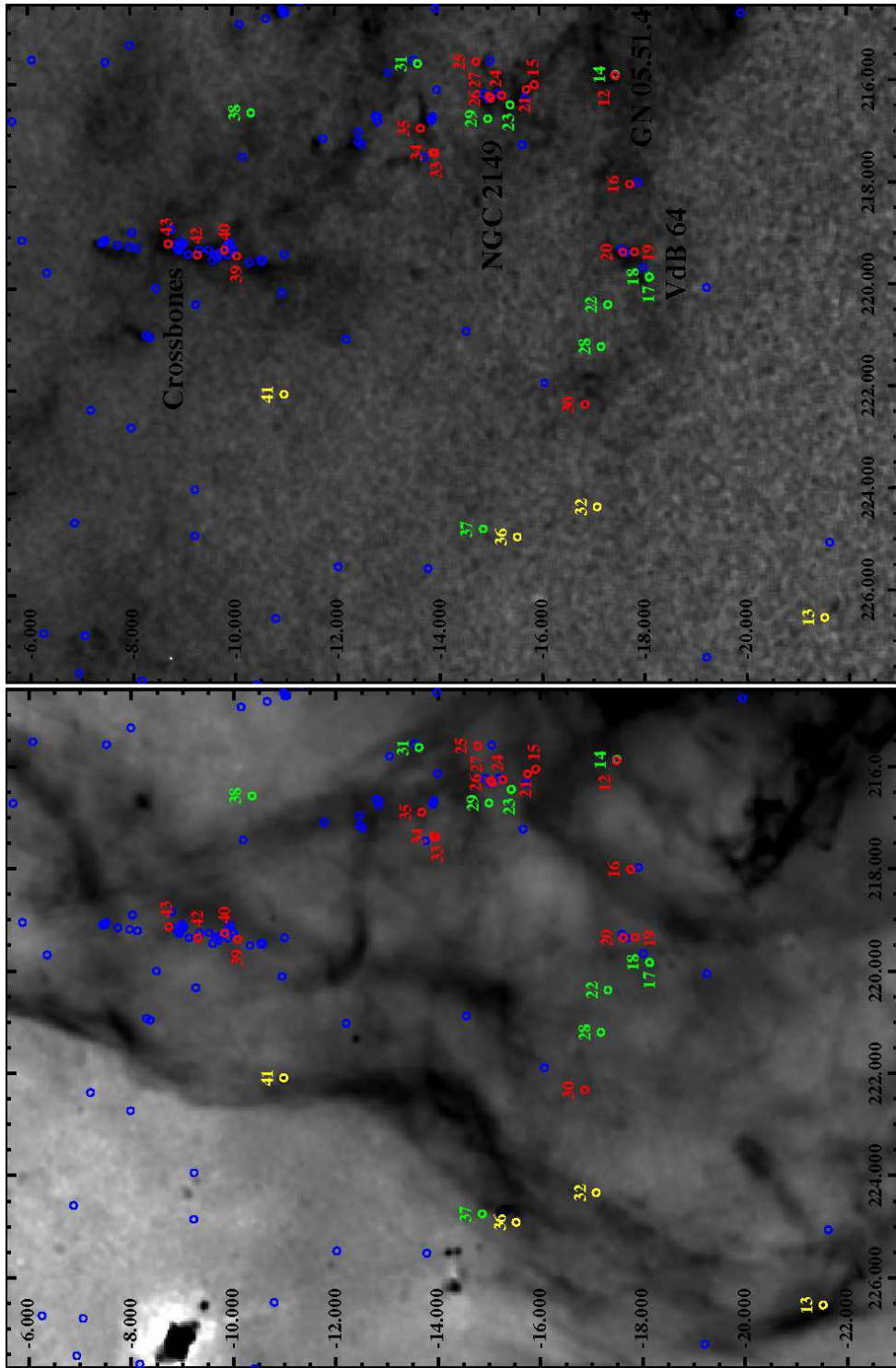


Fig. 3.— Same as Fig. 2, but for the Region Two.

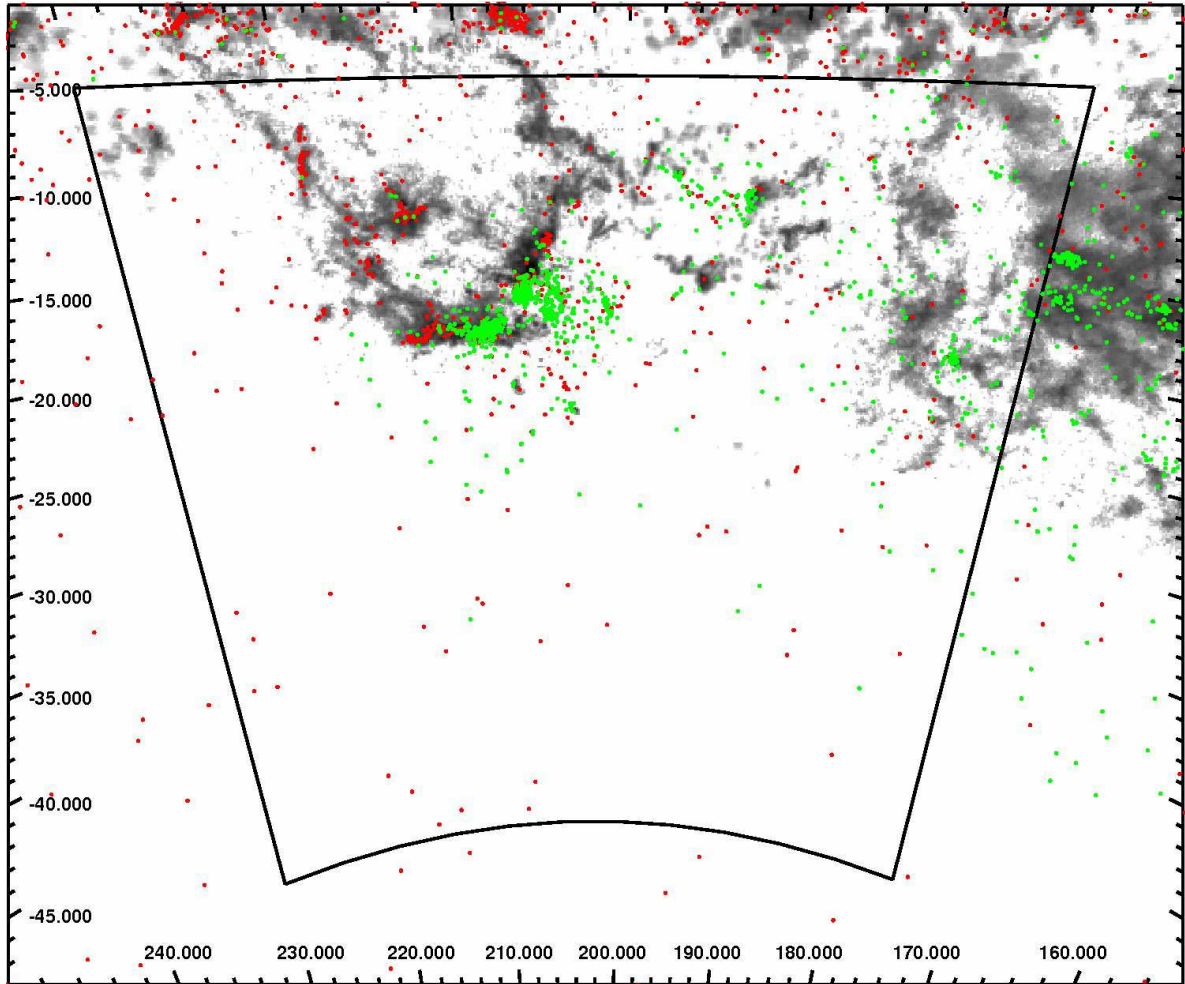


Fig. 4.— Young stellar objects from SIMBAD (green dots) and our sample (red dots) including CTTS and HAeBe stars. SIMBAD objects are distributed over the Orion region and LDN 1551. However, our sample reveal star formation in less explored regions, NGC 2149, VdB 64, and the Crossbones. Solid lines indicate the region studying in this paper.

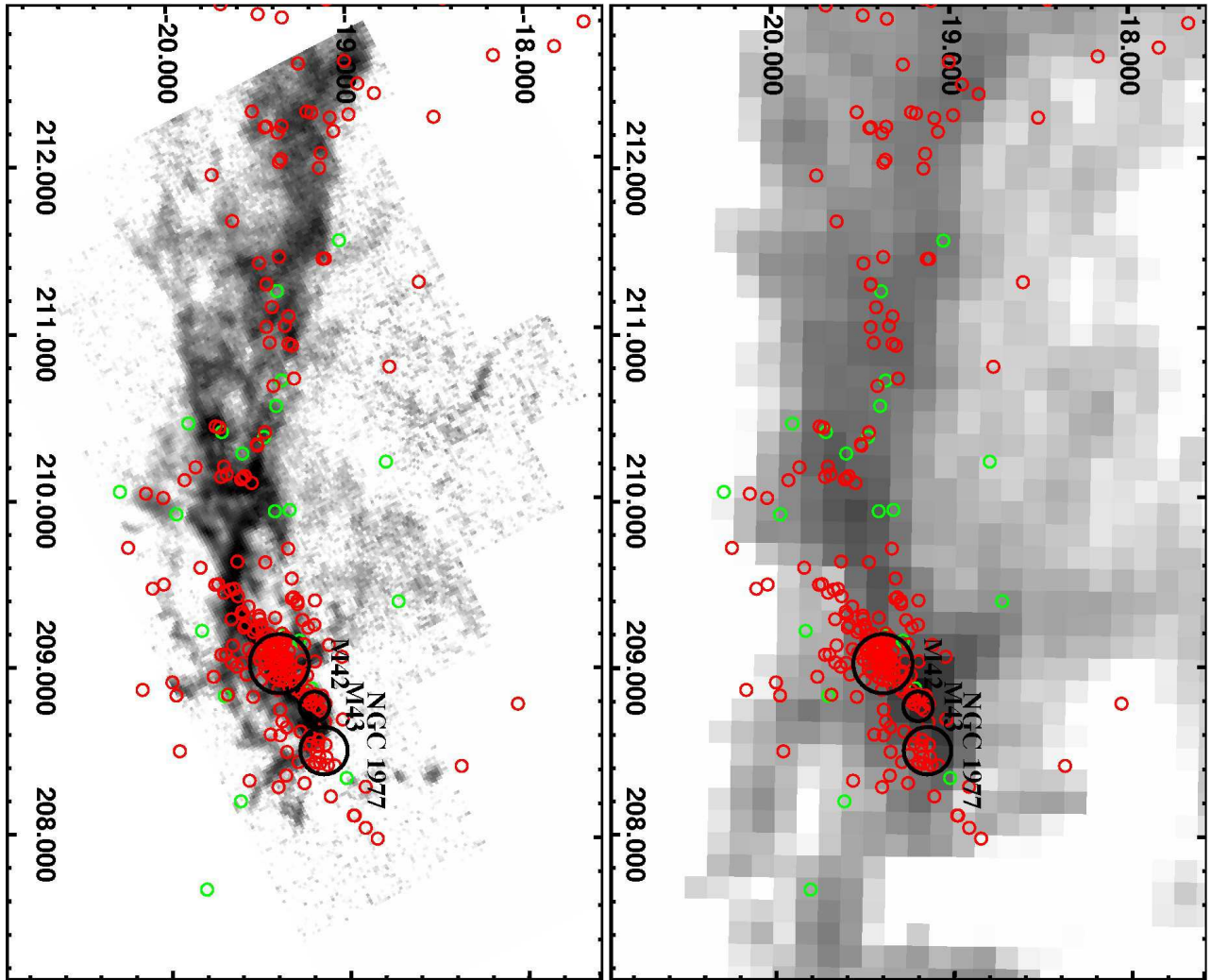


Fig. 5.—  $^{12}\text{CO}$  (top, Dame et al. (2001)) and  $^{13}\text{CO}$  (bottom, Bally et al. (1987)) images of the Orion A molecular cloud in Galactic coordinates. The red and green dots are CTTSs and H AeBe candidate stars, respectively, which are selected by their near-infrared colors.

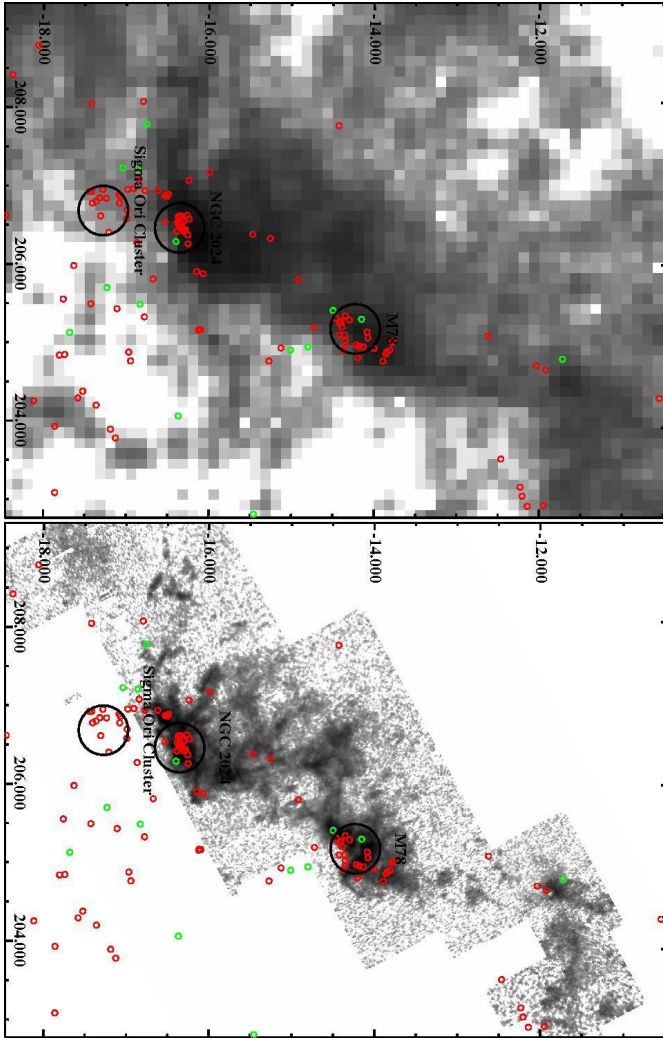


Fig. 6.— Same as Fig. 5,  $^{12}\text{CO}$  (left, Dame et al. (2001)) and  $^{13}\text{CO}$  (right, (Miesch & Bally 1994)), but for the Orion B molecular cloud.

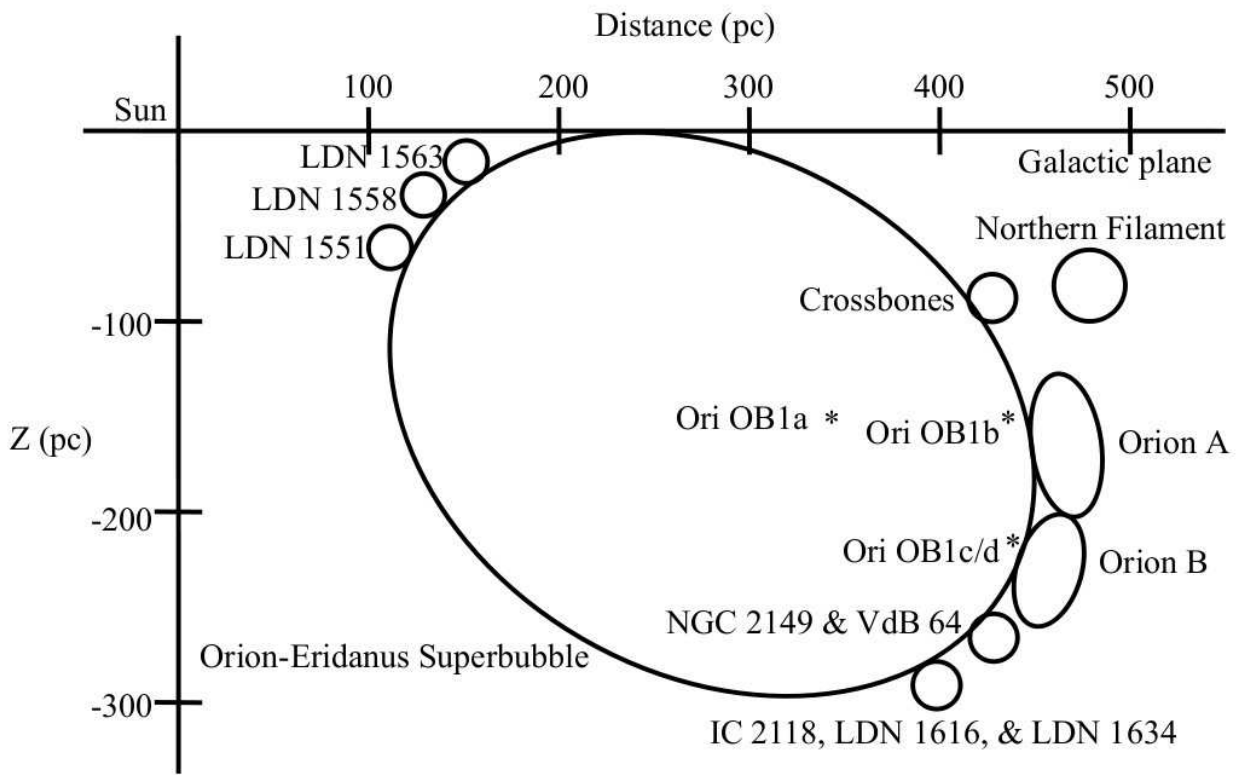


Fig. 7.— Sketch of the Superbubble, approximately to scale. The shape of the Superbubble, the relative positions of clouds, and Ori OB1 subgroups are plotted.

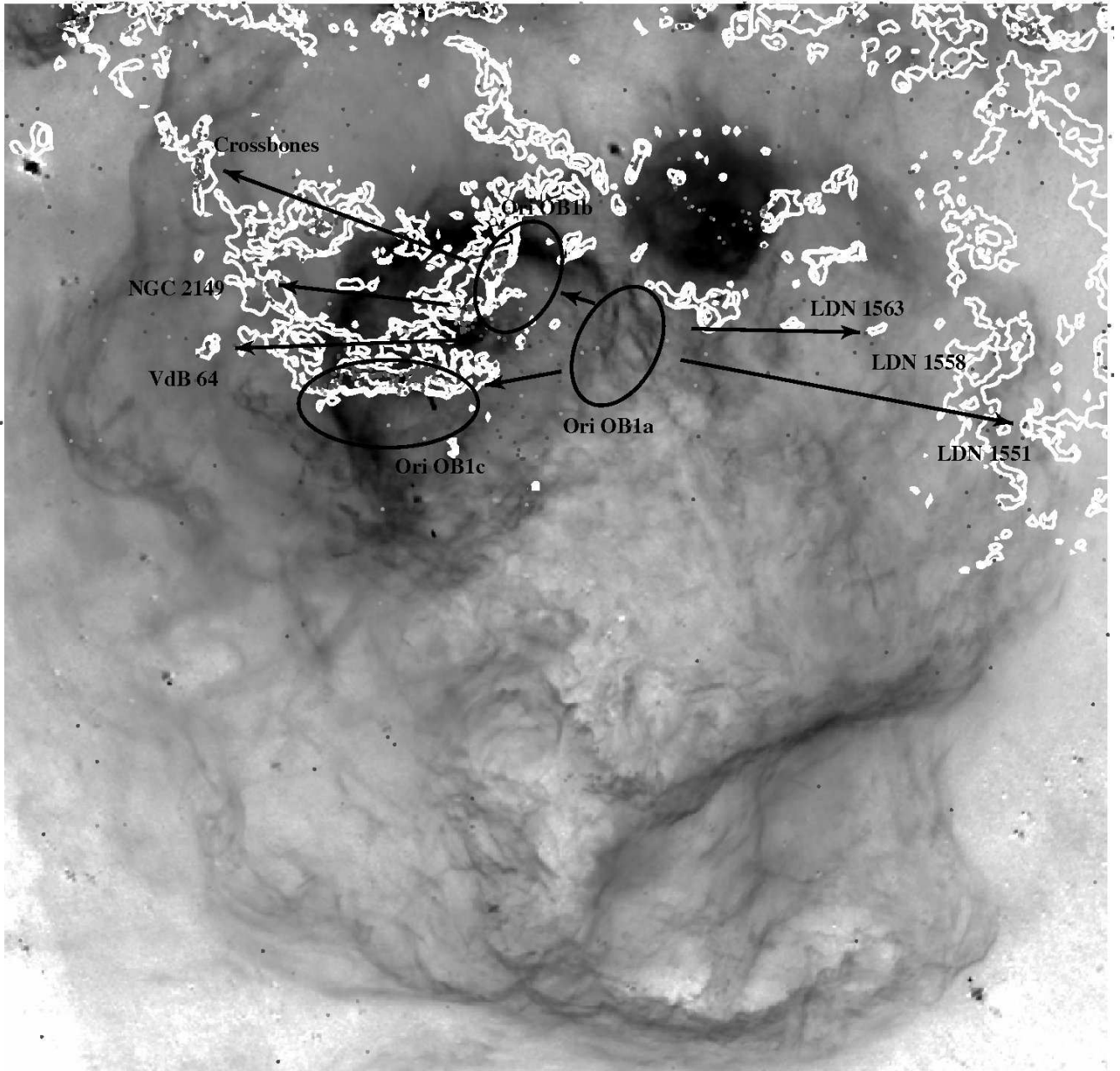


Fig. 8.— Star formation history inside of the Orion-Eridanus Superbubble. Star formation starts from Ori OB1a and propagates to 1b, 1c, and eventually to 1d. The Superbubble spreads star formation to NGC 2149, VdB 64, and the Crossbones, and furthermore also initiates star formation two hundred pc away from Ori OB1a in the LDN 1551, LDN 1563, and LDN 1558 molecular clouds. The grayscale and contours represent the  $H\alpha$  and  $^{12}\text{CO}$  emission, respectively. The symbols for stars are the same as in Figure 1.